Electronic Supporting Information

Super-resolution imaging-based single particle tracking reveals dynamics of nanoparticle internalization by live cells

Yiming Li,[a,b] Li Shang,[a,b] and G. Ulrich Nienhaus[a,b,c,d,*]

[a] Institute of Applied Physics, Karlsruhe Institute of Technology (KIT), Wolfgang-Gaede-Str. 1, 76131 Karlsruhe, Germany

[b] Institute of Nanotechnology, Karlsruhe Institute of Technology (KIT), Hermann-von-Helmholtz-Platz 1, 76344 Eggenstein-Leopoldshafen, Germany

[c] Institute of Toxicology and Genetics, Karlsruhe Institute of Technology (KIT), Hermann-von-Helmholtz-Platz 1, 76344 Eggenstein-Leopoldshafen, Germany

[d] Department of Physics, University of Illinois at Urbana-Champaign, Urbana, IL 61801

[*] Correspondence should be addressed to G. U. N. (uli@uiuc.edu).

Materials and Methods

Direct coupling of transferrin (Tf) to PS40 NPs. 96 μL of 1 μM carboxylated polystyrene nanoparticle (PS40, 40 nm nominal diameter, Ex/Em: 660/680 nm, Invitrogen, Grand Island, NY) suspension were mixed with 304 μL of 2-(N-morpholino)ethanesulfonic acid buffer (MES, 50 mM, pH 6.0) and added dropwise, while shaking, to 400 μL of Tf (freeze-dried powder, Sigma-Aldrich, St. Louis, USA) dissolved in MES buffer at a concentration of 5 mg/mL. 4 mg of 1-ethyl-3-(3-dimethylaminopropyl)carbodiimide (EDAC) were freshly dissolved in 20 μL MES buffer and added to the suspension. The particle-Tf solution was kept for 2 h in the dark, and then purified by three dialysis runs of 24 h each against phosphate buffered saline (PBS, Invitrogen, pH 7.4) solution at 4 °C. Note that the coupling is heterogeneous because there are many amino groups on the protein that may bind to carboxyl groups on the NPs. Also, proteins may crosslink, so the Tf coating on the PS40 NP surface may not be a monolayer.

Coating of PS40 NPs with PEG(10k)-Tf. Tf was dissolved in degassed PBS at a concentration of 5 mg/mL. 20 μL PEGylated N-succinimidyl S-acetylthioacetate ($SAT(PEG)_4$, 1 mg/mL, Thermo Fisher Scientific, Langenselbold, Germany) in dimethyl sulfoxide was added to 1 mL of this solution. After 30 min shaking at room temperature, 100 μL deacetylation buffer (0.5 M hydroxylamine, 25 mM ethylenediaminetetraacetic acid (EDTA) in PBS) was added. After 2 h reaction while shaking, tris(2-carboxyethyl) phosphine (TCEP) (1 mM) was added and incubated for 5 min. Then, the solution was run through a Sephadex G25 spin column in deoxygenated HEPES buffer (pH 7.4). A PS40 NP suspension (10 mg/ml) was added dropwise to a stirring equal volume solution of MAL-PEG-NH_2 linker (M.W. = 10 kDa, 10 mg/mL, Creative PEGWorks, Winston-Salem, NC), both in MES buffer (50 mM, pH 6.0). EDAC (final concentration 1 mg/ml) was added to the suspension and the reaction was allowed to proceed under stirring for 2 h. Following the reaction, the suspension was purified by a Sephadex G25 column with PBS buffer. The resulting suspension was

added to the suspension of SAT(PEG)$_4$ modified Tf. Following another 2 h of reaction, the NP suspension was purified by three dialysis runs against PBS at 4 °C for 24 h each.

Labeling Tf with Alexa 647. 50 µL of 1 mg/mL Tf solution in PBS were mixed with 40 µL of PBS, 1 µL of 2.5 µg/µL Alexa 647 succinimidyl ester (Invitrogen) in DMSO and, subsequently, 10 µL of 1 M $NaHCO_3$ (pH 8.0) were added. The solution was shaken for 30 min at room temperature in the dark. Labeled Tf was purified by gel filtration using Bio-Spin 6 column (Bio-rad, CA, USA). The Tf:dye labeling ratio was determined by using a Nano-drop 2000c spectrometer (Thermo Fisher Scientific) as ~3 dye molecules per Tf. For cellular imaging, COS-7 cells were preincubated in serum-free Dulbecco's modified Eagle's medium (DMEM) for 30 – 60 min at 37 °C. 1 µM Tf-Alexa 647 was added *in situ* and left to incubate for 3 min. Then, the cells were thoroughly rinsed in DMEM for imaging.

Staining of cell membranes and nuclei and spinning disk confocal imaging. COS-7 cells were incubated with 0.5 µg/mL Hoechst 33342 nucleic acid stain in serum-free DMEM for 30 min. Afterwards, membranes were stained with 0.25 µg/mL CellMask™ Orange (Invitrogen) in DMEM for 5 min. Cells were washed twice with PBS and, after adding the same amount of PS NPs as for TIRF imaging, live cell imaging was performed for 1 h in 2 s intervals (50 ms exposure time) by using an Andor Revolution® XD spinning disk laser scanning microscope (BFi OPTiLas, München, Germany) with alternating excitation by 405-nm, 561-nm and 640-nm laser light.

Antibody labeling of CCPs. COS-7 cells transfected with CLC-mEos2 were fixed with 4% paraformaldehyde in PBS for 10 min. After two washing steps with PBS (5 min each), cells were permeabilized with 0.5% Triton X-100 in PBS for 10 min. After washing twice with PBS, the sample was blocked with 5% BSA in PBS for 30 min. Then, the sample was stained with a primary antibody against clathrin (1 µg/µL rabbit anti-clathrin heavy chain, ab 21679, Abcam, Cambridge, UK) in BSA blocking buffer. After overnight incubation at 4 °C, the sample was rinsed with washing buffer (0.1% Tween-20 in PBS) three times (5 min each).

Secondary antibody (Rabbit IgG antibody, Rockland Immunochemicals, Gilbertsville, PA) labeled with Alexa 647 was added to the sample in blocking buffer. 60 min later, the labeled sample was washed three times with washing buffer and imaged in PBS solution.

Inhibitor studies. To observe the effect of chlorpromazine, an inhibitor of clathrin-mediated endocytosis, cells were pre-incubated for 30 min with 10 μg/mL chlorpromazine hydrochloride in serum free DMEM prior to their exposure to NPs. Then, 200 μL of a solution containing the same inhibitor concentration plus PS40 or PS200 NPs (final concentration 20 μg/ml in serum-free DMEM, ~1 nM for PS40 and 0.01 nM for PS200) were added to the cells grown in eight-well LabTek chambers and incubated for 2 h. Subsequently, 200 μL of 0.5 μg/mL CellMask™ Orange (Invitrogen) in DMEM were added to the COS-7 cells and incubated for 5 min. The cells were washed three times with PBS before imaging. For a quantitative analysis of NPs uptake, we acquired dual-color spinning disk confocal images at cross sections ~2 μm above the bottom membrane. For each cell, the fluorescence intensity of the internalized PS NPs was quantified by dividing the integrated intensity by the cell area.[1] By using ImageJ software, the intracellular region was identified manually, based on the membrane staining.

Cell culture. COS-7 cells were cultured at 37 °C and 5% CO_2 in Dulbecco's modified Eagle's medium (DMEM, Invitrogen, Grand Island, NY), supplemented with 10% fetal bovine serum, 100 U of penicillin, and 100 μg/mL streptomycin. Cells were seeded in eight-well LabTek chambers (Nunc, Langenselbold, Germany) to 50% confluence. One day after seeding, cells were transfected with a plasmid encoding CLC-mEos2 (gift of Professor X. Zhuang, Harvard University) using promofectin (PromoCell, Heidelberg, Germany) according to the manufacturer's protocol. COS-7 cells were incubated with serum-free DMEM for 30 min, which was then exchanged for DMEM containing carboxylated PS NPs (Fluospheres, dark red 660/680, Invitrogen) at a concentration of 0.5 nM. Only for PS40-Tf NPs, 20 nM was applied due to their low binding affinity to the cell membrane.

Fluorescence imaging. Images were acquired at 37 °C on a modified inverted microscope (Zeiss Axio ObserverZ1, Jena, Germany) equipped with a high-NA oil immersion objective (Zeiss alpha Plan-Apochromat 63x/1.46 Oil Corr M27). Four solid-state lasers with wavelengths 640 nm (OXX-LBX, Laser 2000, Wessling, Germany), 561 nm (GCL-150-561, CrystaLaser, Reno, NV), 473 nm (LSR473-200-T00, Laserlight, Berlin, Germany) and 405 nm (CLASII 405-50, Blue Sky Research, Milpitas, CA) were employed for excitation and photoactivation of the fluorophores. The laser beams were combined via dichroic mirrors (AHF, Tübingen, Germany) and guided through an AOTF (AOTFnC-400.650, A-A, Opto-Electronic, Orsay Cedex, France) to control the laser intensity at the sample. Both CLC-mEos2 and PS NPs were excited by the 561 nm laser. An additional neutral density filter was added in the NP detection channel to avoid saturation of the EMCCD camera (iXon DU-897, Andor, Belfast, UK). mEos2 fluorescent protein was converted from its green to its red emitting form by using 405-nm irradiation. 5,000 frames with an exposure time of 30 ms each were taken. For two-color imaging of mEos2 and dark red fluorescent PS NPs, the fluorescence was first passed through a 561 nm long pass filter. Fluorescence emission from mEos2 and PS was separated by a 640 nm short pass dichroic mirror mounted on a commercial beam splitting device (OptoSplit II unit, Cairn Research, Kent, UK). The short wavelength channel was filtered with a dual bandpass filter (HC 523/610, AHF) for mEos2. For PS200 NPs, a bandpass filter (560/50 nm, center wavelength/width) was used instead of the dual bandpass filter to avoid cross-talk of PS200 into the short wavelength channel. The long wavelength channel was filtered with a band pass filter (HC 697/75, AHF). Cross-talk between the two channels was negligible even though the fluorescence intensity from the PS NPs was much higher than the one from mEos2 (Supporting Information, Fig. S21).

Quantitative Image Registration. The positions of the NPs in the individual frames were linked to create trajectories in the long wavelength channel; the PALM image of the CCPs was reconstructed in the short wavelength channel as described.[2] We overlaid the trajectories

and the PALM images, acquired simultaneously with the same camera, using a mapping function derived from measurements on a fluorescent bead sample. This sample was prepared by adsorbing a dilute aqueous solution of ~100 nm Tetraspeck fluorescent beads (~0.3 pM, Invitrogen) on poly-L-lysine coated glass cover slips. The bead density was chosen such that about 50 – 80 beads were visible in the field of view (Supporting Information, Fig. S2). Images of different regions of the sample were acquired to randomly sample the field of view. For each image, locations which appeared in both channels were identified; these pairs are called control points. A mapping function based on this set of control points was calculated and applied to all other data points. We used local weighted mean (LWM) mapping in this work:[3]

$$f(x,y) = \frac{\sum_i W_i(R) P_i(x,y)}{\sum_i W_i(R)},$$

where the local weight, $W_i(R)$, is defined as:

$$W_i(R) = 1 - 3R^2 + 2R^3 \qquad 0 \le R \le 1$$

$$W_i(R) = 0 \qquad R > 1$$

and

$$R = \frac{\left[(x - x_i)^2 + (y - y_i)^2\right]^{1/2}}{R_n}.$$

Here, R_n is the distance of position (x, y) to the n-th closest control point. P_i (x, y) is a quadratic mapping function of control point i based on its n nearest control points. We obtained best results with n = 400.

The target registration error (*TRE*) was used to estimate the mapping error,

$$TRE = \left(\frac{1}{N}\sum_{i=1}^{N}\left(X_{i,1} - T_i\left\{X_{i,2}\right\}\right)^2\right)^{1/2},$$

where N is the number of control points, $X_{i,1}$ and $X_{i,2}$ denote pair i of control points in channel 1 and channel 2, respectively; T_i is the LWM mapping function from channel 2 to 1 without control point i.

Image analysis for particle tracking. Individual NPs were identified by using previously described methods.[2] Briefly, a P value (P = 1 – normal cumulative distribution function) was calculated for each pixel, based on the standard deviation and the mean background of its surrounding region. The P value is a measure of the probability of a pixel to be part of the surrounding background. Local maxima with $P < 0.04$ were selected as molecule candidates. After cropping images of individual molecule candidates, they were fitted to two-dimensional Gaussians to obtain the centroid coordinates using maximum likelihood estimation.[4] The position of each molecule was passed to a tracking program (The Matlab Particle Tracking Code Repository, http://physics.georgetown.edu/matlab/) written in Matlab (The Mathworks, Natick, MA). Only trajectories longer than 1.5 s, corresponding to 50 frames, were used for further analysis.

Trajectory analysis. To characterize NP motion, we performed a moment scaling spectrum (MSS) analysis.[5] Moments of displacements are defined by

$$u_\nu(\delta t) = \left\langle \left| \mathbf{R}(t+\delta t) - \mathbf{R}(t) \right|^\nu \right\rangle,$$

where $\mathbf{R}(t)$ is the position vector at time t, δt is the time shift, $\nu \in \mathrm{N}$, is the order of the moment. The special case $\nu = 2$ is called the mean square displacement (*MSD*). Normal diffusion is characterized by $u_2 \propto \delta t^1$, and the proportionality factor is given by twice the diffusion coefficient, D, per spatial dimension. For anomalous diffusion, however, $u_2 \propto \delta t^{\gamma_2}$, with $\gamma_2 \neq 1$, which can also be expressed by keeping an explicitly linear time dependence but introducing a time-dependent $D(t)$.

Moments up to order six were calculated from the NP trajectories. Assuming that each moment obeys a power law, $u_\nu \propto \delta t^{\gamma_\nu}$, the scaling coefficients γ_ν were determined by linear regression of double-logarithmic plots of u_ν versus δt. Here, the value of $D(t)$ at 1 s, D_0, was obtained from the y-axis intercepts, y_0, of the second order as: $D_0 = ¼ \exp(y_0)$. The plot of γ_ν versus ν is called the moment scaling spectrum, *MSS*.[6] It shows a straight line through the origin for all strongly self-similar processes, with a slope, S_{MSS}, that characterizes the modes of motion within the same trajectory. S_{MSS} values of 0, 0.5 and 1 correspond to immobilization, free diffusion and directed transport with constant velocity, respectively. S_{MSS} values between 0 and 0.5 are associated with confined diffusion (subdiffusion), and those between 0.5 and 1 are associated with superdiffusion.

Microscopic diffusion coefficients. Microscopic diffusion coefficients of individual tracks, denoted by $D_{1\text{-}4}$, were determined by linear fits to the *MSD* of the first four image frames, corresponding to an elapsed time of 120 ms for our data. For diffusion in compartmentalized space, $D_{1\text{-}4}$ characterizes short-term diffusion within a compartment, whereas the long-term behavior is governed by the dynamics across many compartments. $D_{1\text{-}4}$ is a convenient parameter because it can be determined independently of the motional modes.[7]

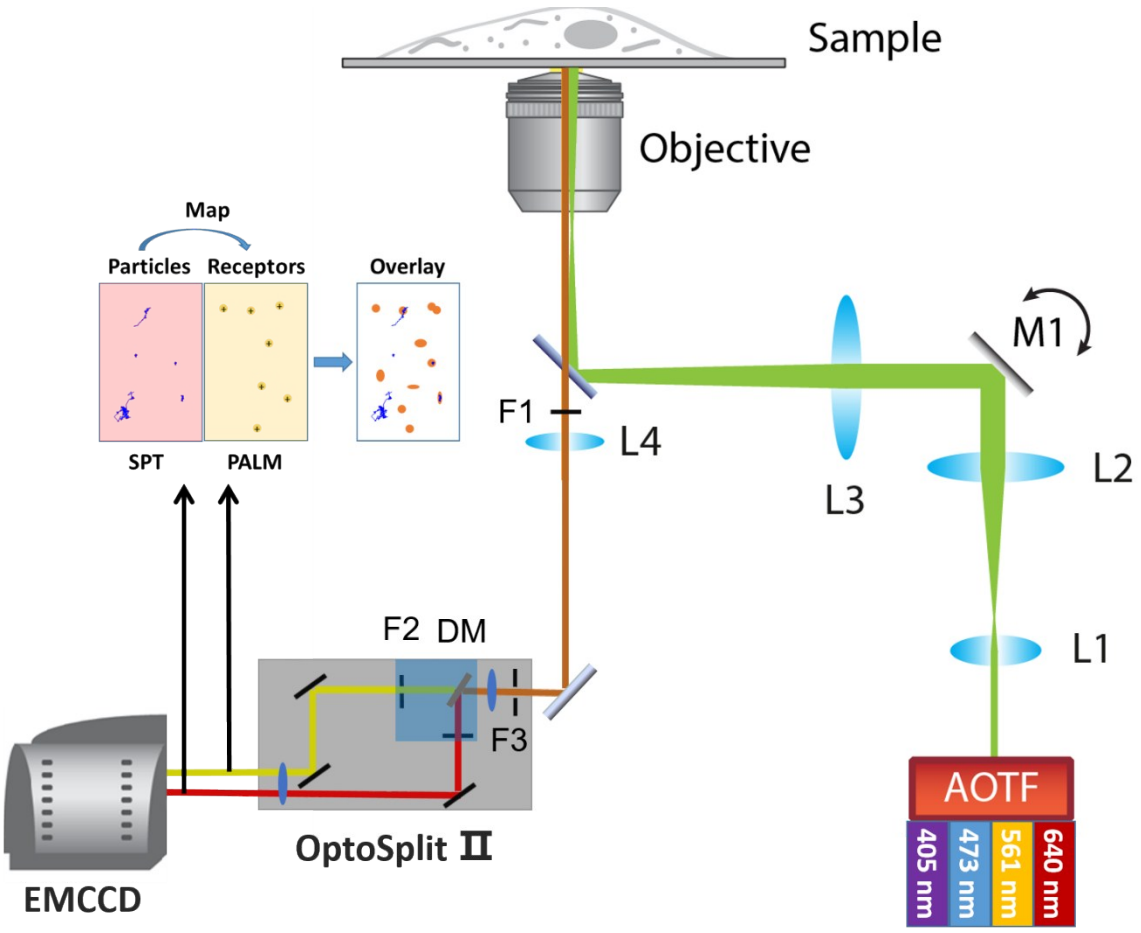

Fig. S1 Schematic of the widefield microscope used for localization microscopy and single particle tracking. Light emitted by four solid-state lasers is combined and guided through an AOTF. A telescope (lenses L1 and L2) allows the size of the illuminated spot on the sample to be adjusted. Lens L3 focuses the laser beam on the back focal plane of the objective to generate widefield illumination. A movable mirror (M1) allows beam steering to operate the microscope in TIRF, inclined illumination, or widefield mode. The emitted fluorescence is collected by the objective and passed through a 561 nm long pass filter F1. After traversing the tube lens L4, the fluorescence is separated by a 640-nm short-pass dichroic DM in a commercial beam splitting device (OptoSplit II, Cairn Research, Kent, UK). The short wavelength channel is filtered with dual-band filter F2 (HC 523/610, AHF, Tübingen, Germany) for mEos2. The long wavelength channel is filtered with a band pass filter F3 (HC 697/75, AHF). The long-pass filter F1 is removed for TIRF imaging of green emitting CLC-mEos2 prior to photoconversion to the red form using 405-nm light.

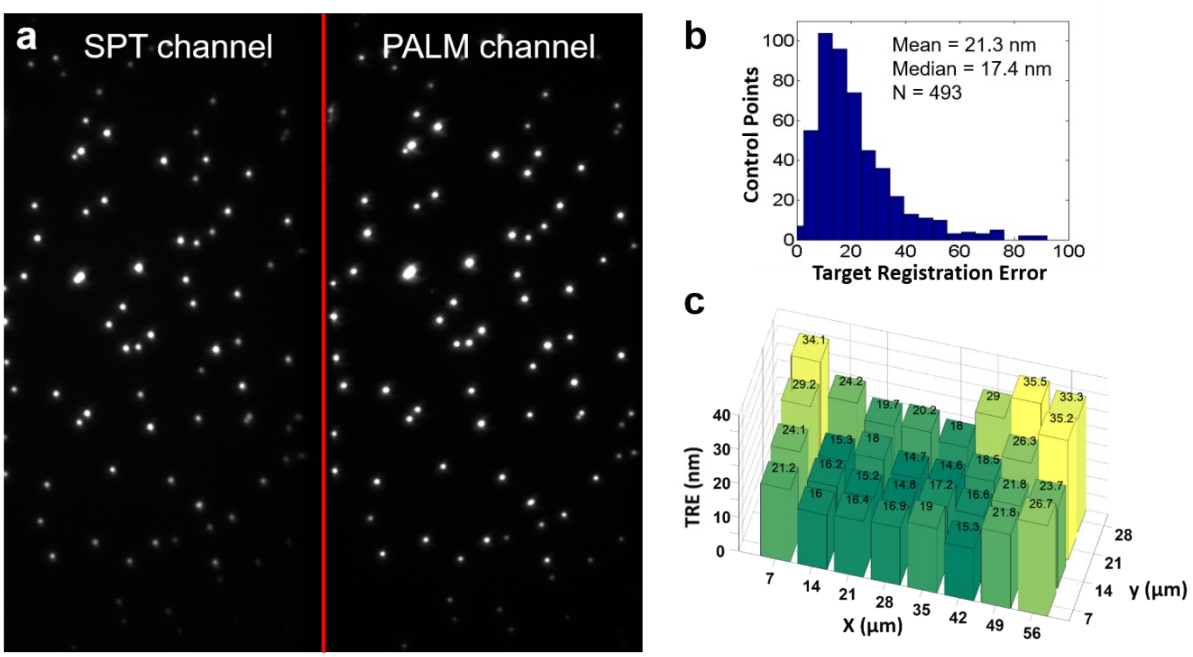

Fig. S2 Accurate image registration using multicolor beads. a, Images of beads as acquired in the SPT and PALM color channels. The bead density was chosen such that ~50 – 80 beads were visible in the field of view. b, The target registration error (*TRE*) was computed for each control pair by iteratively removing a given control pair and computing the mapping function with the remaining control pairs. The mapping function was calibrated before each experiment. c, Distribution of mean *TRE*s for different sub-regions of the field of view. In the central area, the *TRE* is lower than in the periphery due to spherical aberrations of the optical system.

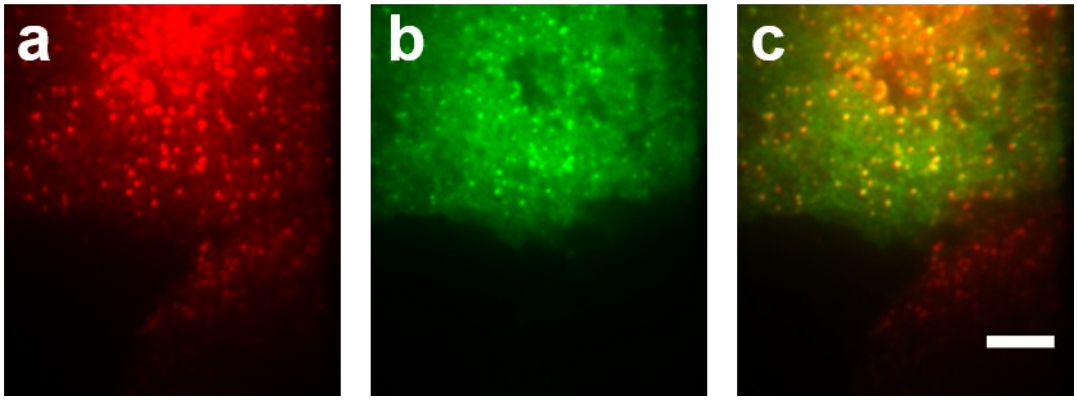

Fig. S3 Dual-color TIRF image of a fixed COS-7 cell expressing CLC-mEos2. a, The image in the red channel shows CCPs visualized by immunostaining with an anti-clathrin heavy chain primary antibody and an Alexa 647-labeled secondary antibody. b, The image in the green channel shows CCPs *via* mEos2 fluorescence. c, Overlay of the two color channels, so puncta with both red and green emission appear in yellow. Scale bar, 5 μm.

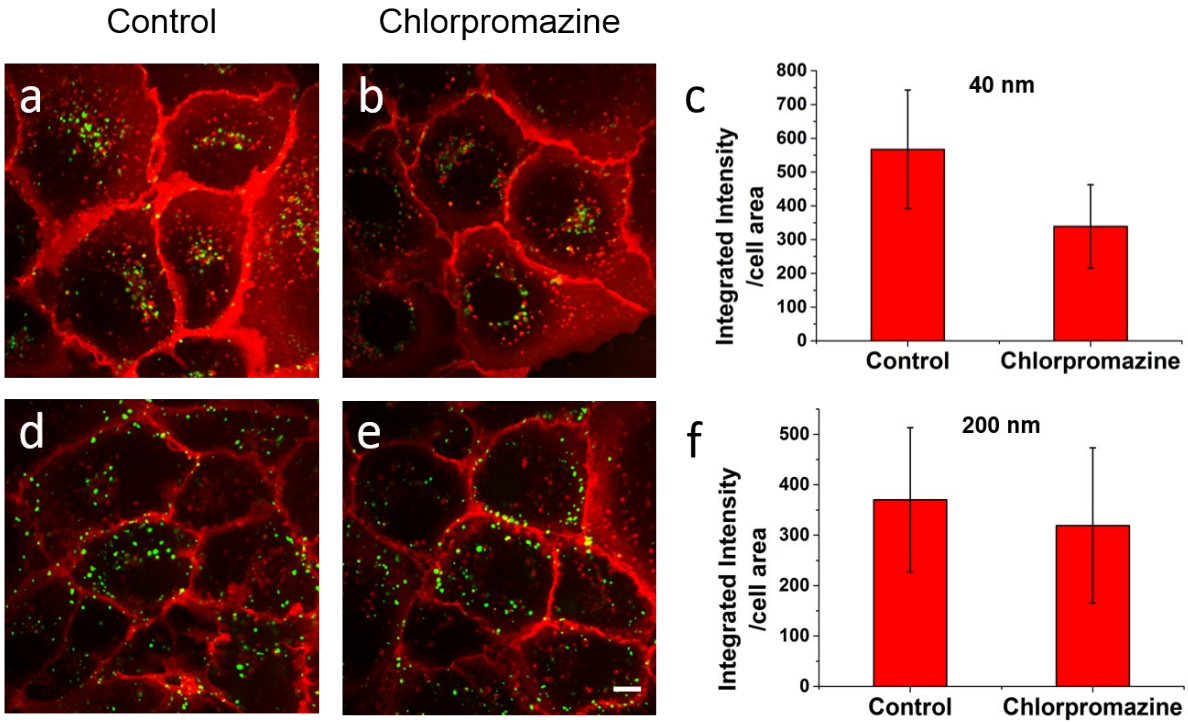

Fig. S4 Effect of chlorpromazine on the uptake of PS40 and PS200 NPs by COS-7 cells. Spinning disk confocal images of COS-7 cells after 2 h incubation with 20 μg/mL PS40 NPs, a, without inhibitor (control) and, b, with 10 μg/mL chlorpromazine. c, Overall uptake of PS40 NPs, averaged over 32 cells, showing that chlorpromazine suppressed uptake by ~40%. Spinning disk confocal images after 2 h incubation with 20 μg/mL PS200 NPs, d, without inhibitor (control) and, e, with 10 μg/mL chlorpromazine. f, Overall uptake of PS200 NPs, averaged over 25 cells. Within the error, there is no indication of suppressed PS200 NP internalization due to chlorpromazine. Scale bar, 10 μm.

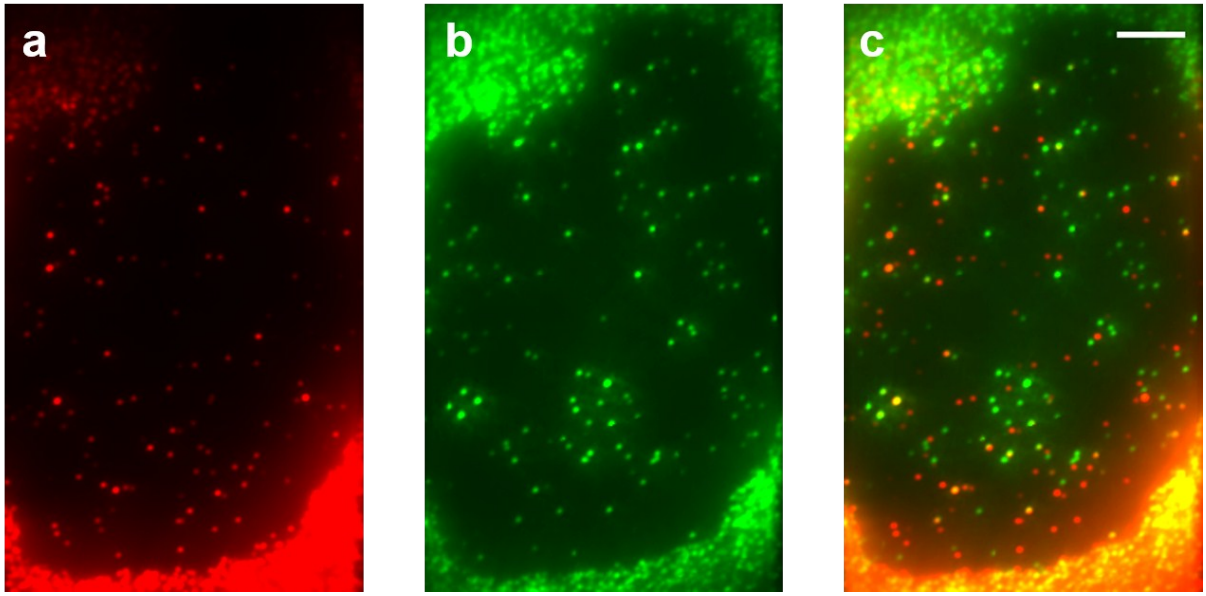

Fig. S5 Dual-color TIRF image of a COS-7 cell exposed to a 1:1 mixture of differently colored PS40 NPs. Cells were incubated with NPs for 40 min and then fixed for imaging, which ensures that NPs only weakly adhering to cells are removed. NPs with excitation/emission peaks at 580/605 nm, which we refer to here as 'green NPs', were excited by laser light at 561 nm; red NPs (excitation/emission peaks at 660/680 nm) were excited by laser light at 640 nm. **a,** Red PS40 NPs at the bottom surface of a COS-7 cell, imaged with a band pass filter (HC 697/75, AHF). b, Same view in the green channel, filtered with a band pass filter (HC 582/75, AHF). c, The two images were merged using the image registration method described in Supplementary Methods and Fig. S2. Scale bar, 5 µm. By analyzing images from eight cells, we identified 389 green, 387 red and 194 green-red spots, yielding a degree of colocalization of 33% for both colors. The NPs were not observed to aggregate, and the predominance of singly labeled spots indicates that only a small number of NPs is associated with a CCP. Obviously, the more NPs congregate in one CCP, the lower is the probability of finding spots with only a single color.

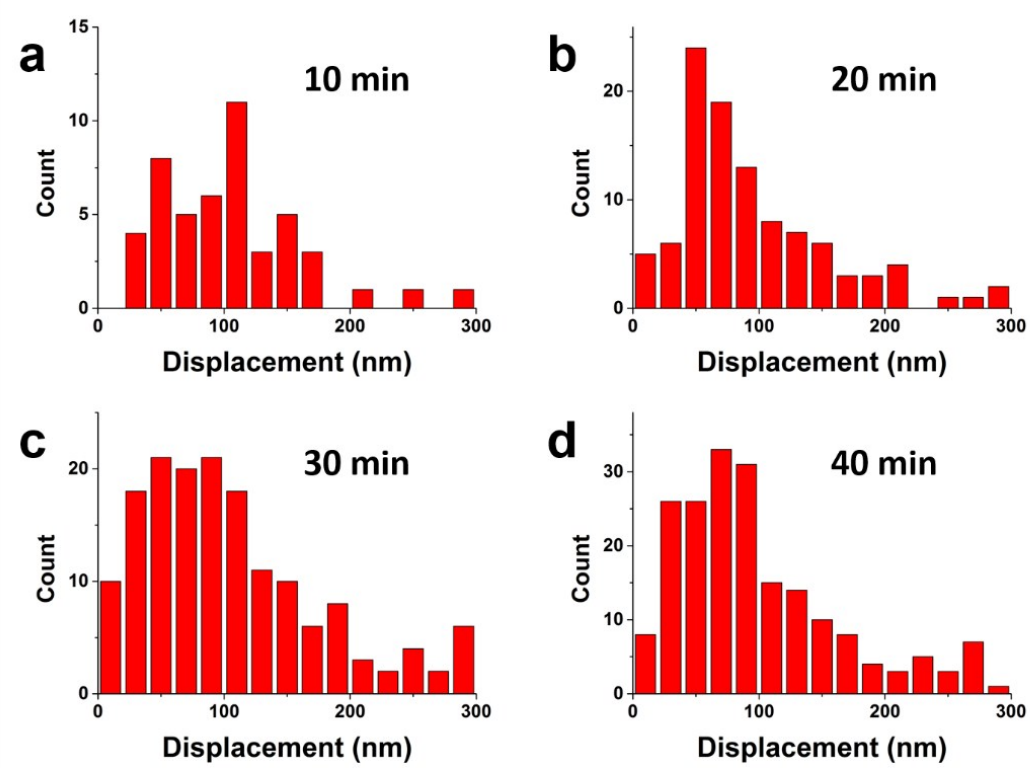

Fig. S6 Displacement of colocalized red and green PS40 NPs. COS-7 cells were fixed at different time points after incubation with a 1:1 mixture of red and green PS40 NPs. The distributions of mutual displacements are displayed in panels a, b, c and d for 10, 20, 30 and 40 min of NP exposure prior to fixing the cells, respectively. The fraction of colocalized NPs, 12% (48/391), 15% (102/683), 18% (160/870), 20% (194/970) for 10, 20, 30 and 40 min of NP exposure, respectively, shows a tendency to saturate over time. The average displacement between differently colored NPs, 105 ± 55 nm, 93 ± 60 nm, 105 ± 70 nm and 98 ± 65 nm (in the order of increasing time), remained constant even though the total number of colocalized NPs increased. This shows that we do not observe larger aggregates, but always only a few NPs residing within each CCP. The calculated displacements allow the NP size to be estimated.[8] For two NPs residing in the image plane, we add the NP diameter (62 nm) to obtain the overall diameter of the cavity, 167 ± 55 nm, 155 ± 60 nm, 167 ± 70 nm and 160 ± 65 nm. Of note, for a random orientation of the vector connecting the center of two beads in three-dimensional space, we only observe a projection into the image plane, so the quoted diameters should be multiplied by a factor of $4/\pi$.

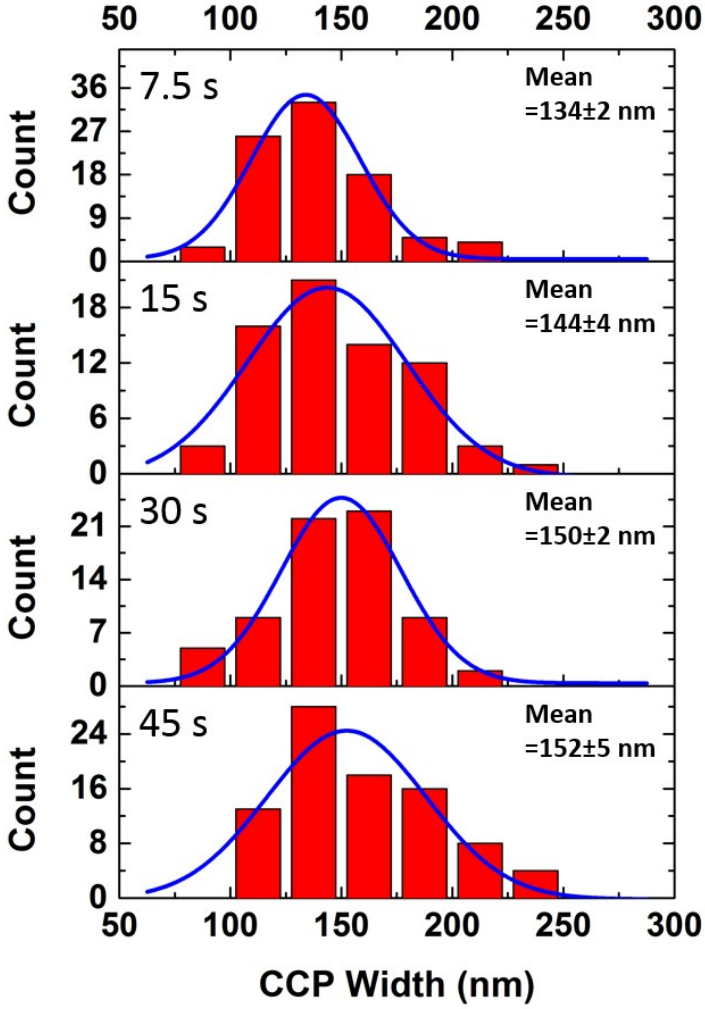

Fig. S7 Apparent size distributions of CCPs obtained from PALM images with different time bins. There are two possible effects influencing the apparent size: (1) CCP movement during the data acquisition gives rise to artificially enlarged sizes; (2) CCPs grow during their lifetime,[9] so that shorter binning time for reconstructing the PALM image tends to underestimate the CCP size. Moreover, a too short time window can lead to an under-estimation of the CCP size due to lack of sufficient molecules to reconstruct the complete CCP structure. The average size of the CCPs using a 30 s snapshot is increased by ~16 nm compared with that at 7.5 s, while larger time bins (*i.e.*, 45 s) do not change the size distribution significantly. A tail toward greater sizes at 45 s indicates that motional effects come into play. Therefore, we chose 30 s binning in our experiments.

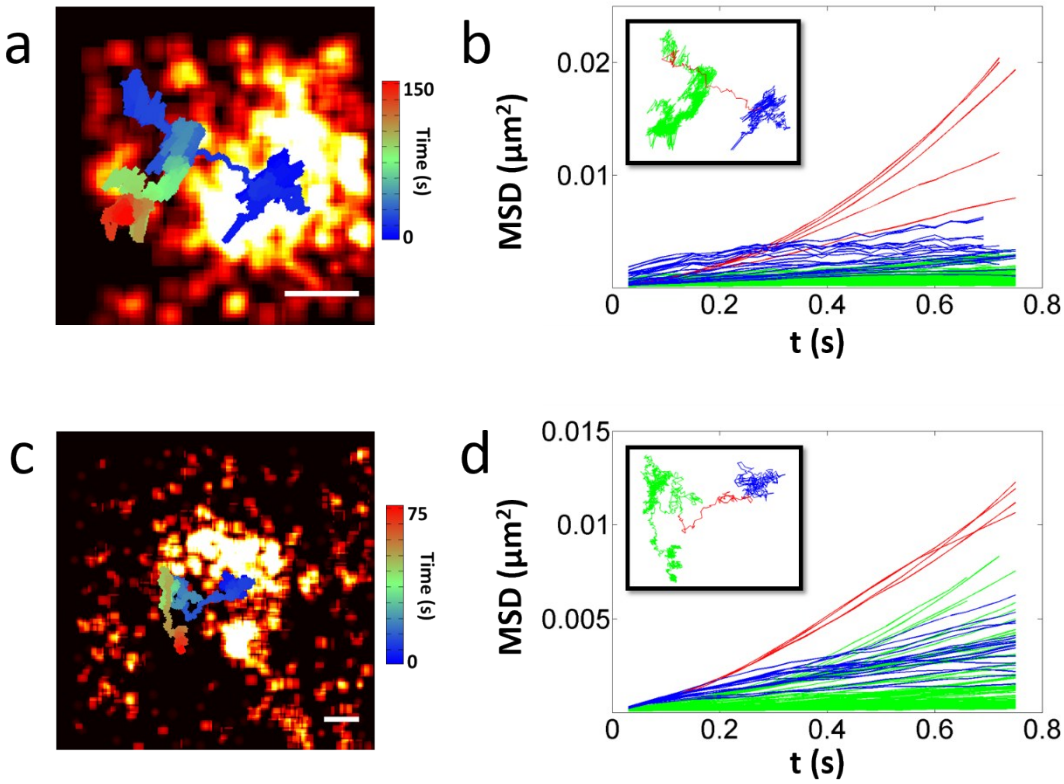

Fig. S8 MSD analysis of PS40 NPs colocalized with CCPs. a, Overlay of a PS40 NP trajectory and a PALM image of a CCP. b, Plots of the local *MSD* functions calculated by using a rolling window algorithm (*i.e.*, time windows of 3 s (100 camera frames) in steps of 0.6 s (20 camera frames))**.** Three phases are distinguished by color, as indicated in the trajectories shown in the inset. c, d, Second example, data analogous to panels a, b, respectively. Directed motion of the PS40 NPs is clearly visible in the upward bending of the red *MSD* lines. These results indicate that the NPs perform diffusive motions while they reside in the CCPs and are also dragged along with the CCPs, presumably by the action of the cytoskeletal network. Scale bars, 200 nm.

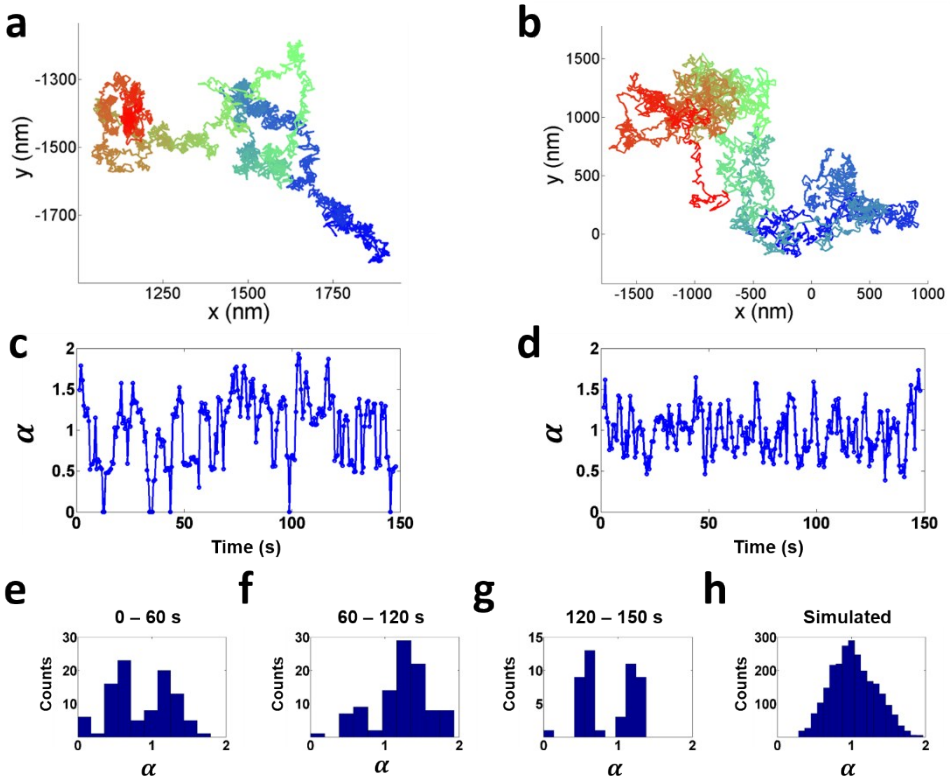

Fig. S9 Time exponent analysis of a measured trajectory of an NP colocalized with a CCP and a simulated trajectory of a particle undergoing Brownian diffusion. a, Experimentally determined and b, simulated (D = 0.01 μm^2/s) trajectory of a NP in time steps of 30 ms, with the time color-coded from blue (0 s) to red (150 s). The local *MSD* function was calculated for time windows of 3 s (100 camera frames) in steps of 0.6 s (20 camera frames) and fitted by a power law function, $MSD = \Gamma t^{\alpha}$ (α = 1 indicates Brownian diffusion, α < 1 anomalous subdiffusion, and α > 1 superdiffusion). c and d are plots of the time exponent α against the time for *MSD* functions calculated from trajectories in panels a and b, respectively. Histograms of α occurrences in the experimental trajectory from e, 0 – 60 s, f, 60 – 120 s, g, 120 – 150 s. h, Histogram of the simulated trajectory (b); it peaks at α = 1 but fluctuates around this value (d) because of the short sampling periods. For the experimental trajectory (c), fluctuations of α are more pronounced, and the histograms (e–g) do not peak at α = 1 but appear bimodal. A stretch of fast displacement in the middle of the experimental trajectory (a) coincides with large α-values, indicating active transport (c, f).

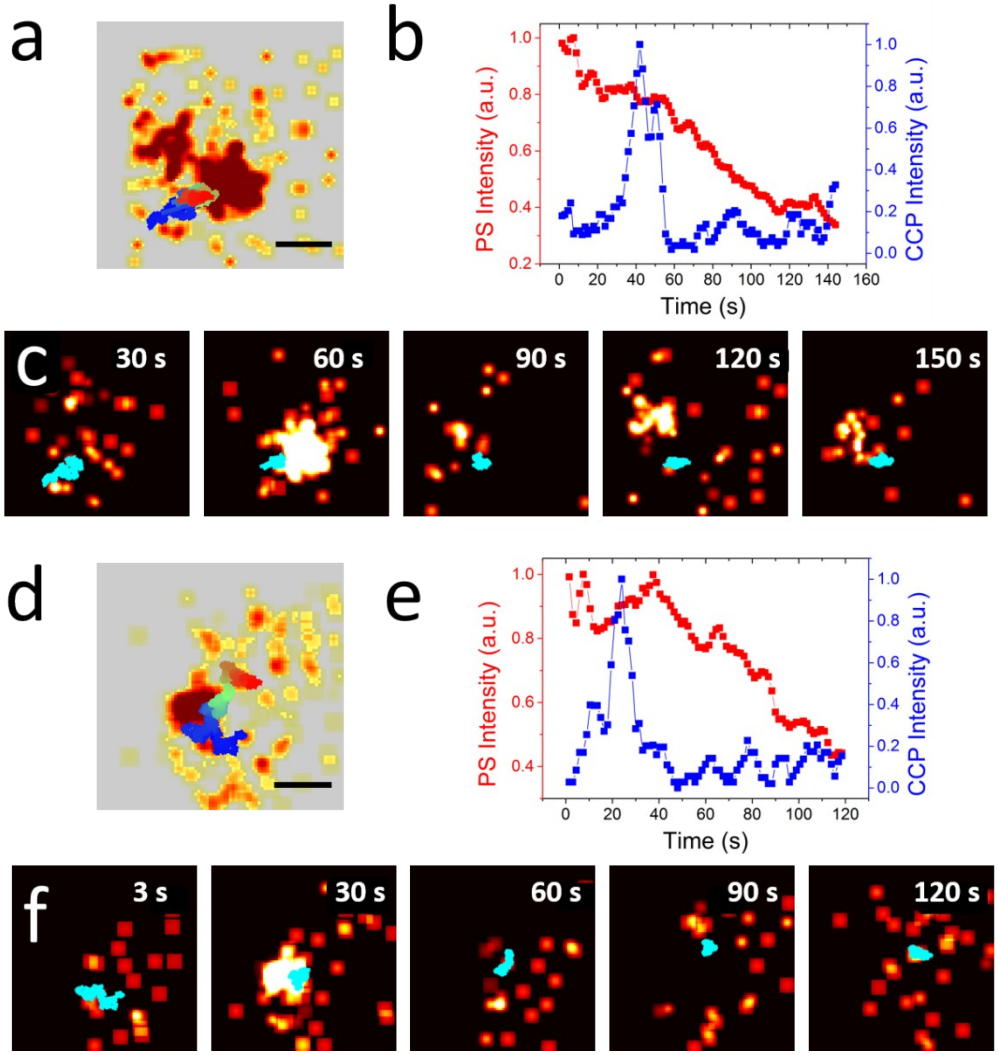

Fig. S10 Two examples of CCPs forming after PS40 NP attachment to the membrane (type I encounter). First example, a, overlay of the entire NP trajectory with a super-resolved PALM image of the CCP. b, Time evolution of the fluorescence intensity of the NP and CLC-Eos2 molecules detected in the CCP during the uptake. For comparison, both data sets were shown normalized. c, Overlay of the NP with the CCP at different times (200 frames per bin). d, e and f are results of the second example, which are analogous to panels a, b and c, respectively. Of note, the NP intensity often did not return to zero even after complete disappearance of the clathrin signal. The decrease by more than 50% indicates, however, that NPs moved away from the surface, *i.e.*, into the cell. Inside the cell, they may not immediately be displaced from the site of internalization. Scale bars, 200 nm.

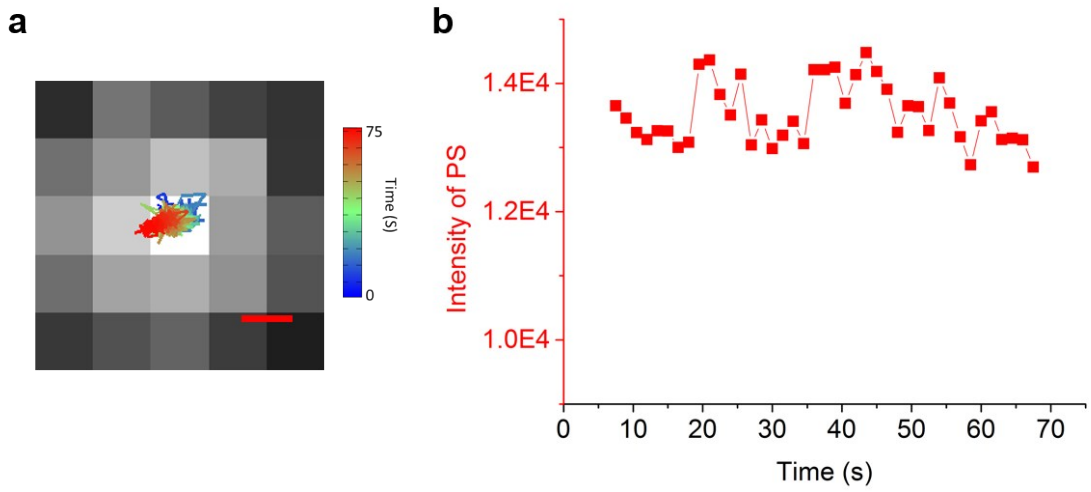

Fig. S11 Trajectory and intensity distribution of a PS40 NP adsorbed onto a glass surface. a, Trajectory of the PS40 NP (center of gravity) on top of the raw data shows a constant location, with standard deviation of 14.7 nm (average). b, The intensity time trace of the NP shows fluctuations around an essentially constant intensity level. Scale bar, 100 nm.

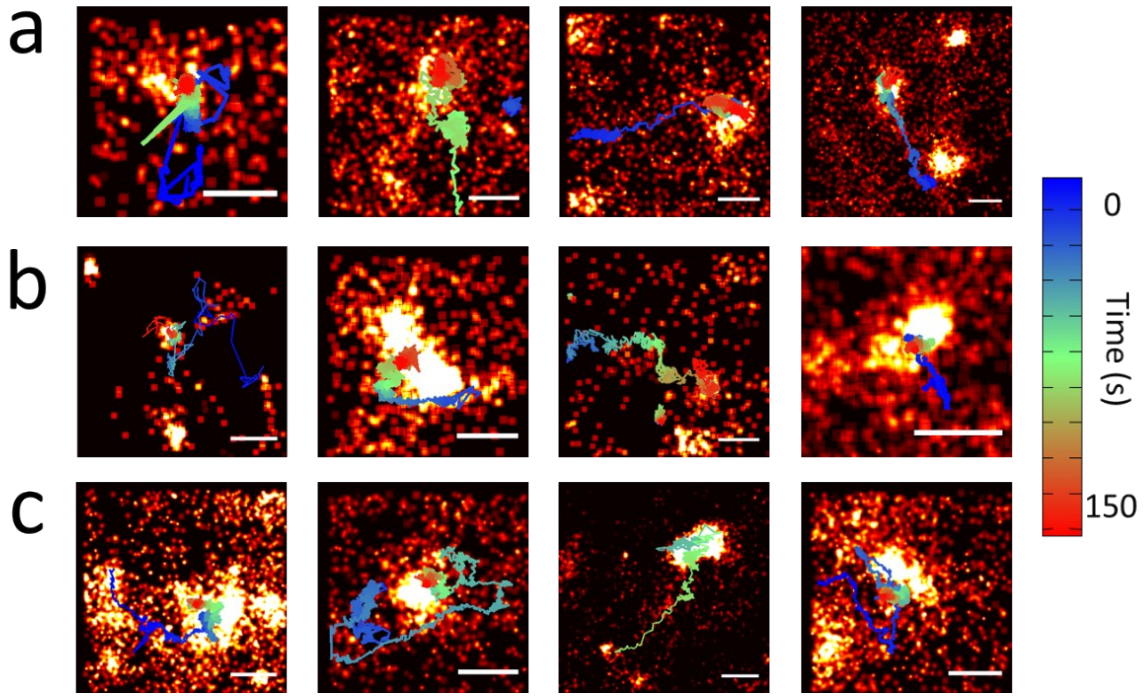

Fig. S12 Examples of PS NPs migrating on the plasma membrane before finding a CCP for internalization (type II encounter). Overlays of a, PS20 NP, b, PS40 and c, PS40-PEG(10k)-Tf NP trajectories with PALM images of CCPs. For PS20, PS40 and PS40-PEG(10k)-Tf NPs, 9% (5/58), 8% (5/63) and 17% (11/64) of all observed colocalization events are classified as type II encounters, respectively. Scale bars, 500 nm.

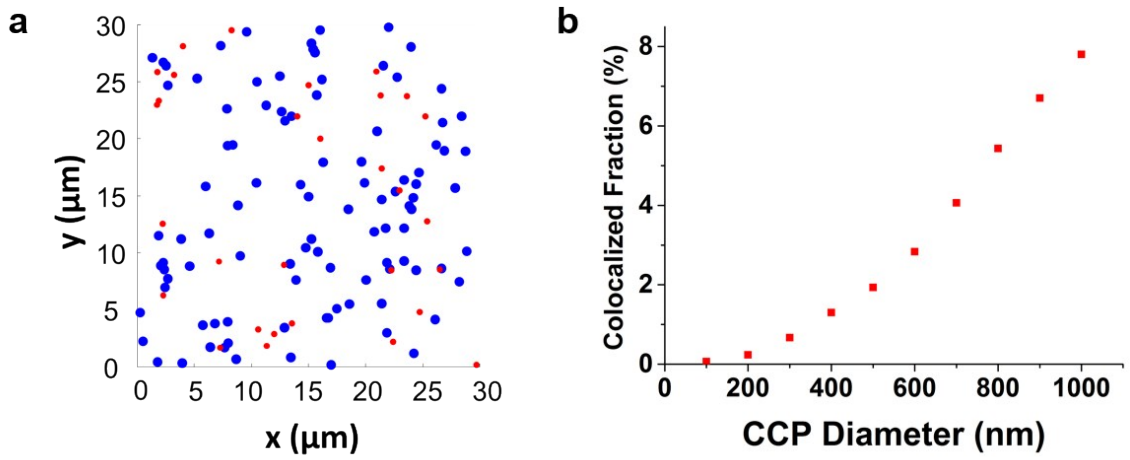

Fig. S13 Simulation of random colocalization of PS NPs and CCPs. a, 30 PS NPs and 100 CCPs were randomly deposited within a field of 30 μm × 30 μm. If the distance between NP locations and the center of CCPs was less than the radius of the CCP, the NP was counted as colocalized. b, Fraction of PS NPs colocalized with CCPs as a function of CCP diameter. For CCPs <200 nm in diameter, only <0.2% of PS NPs are expected to colocalize with CCPs.

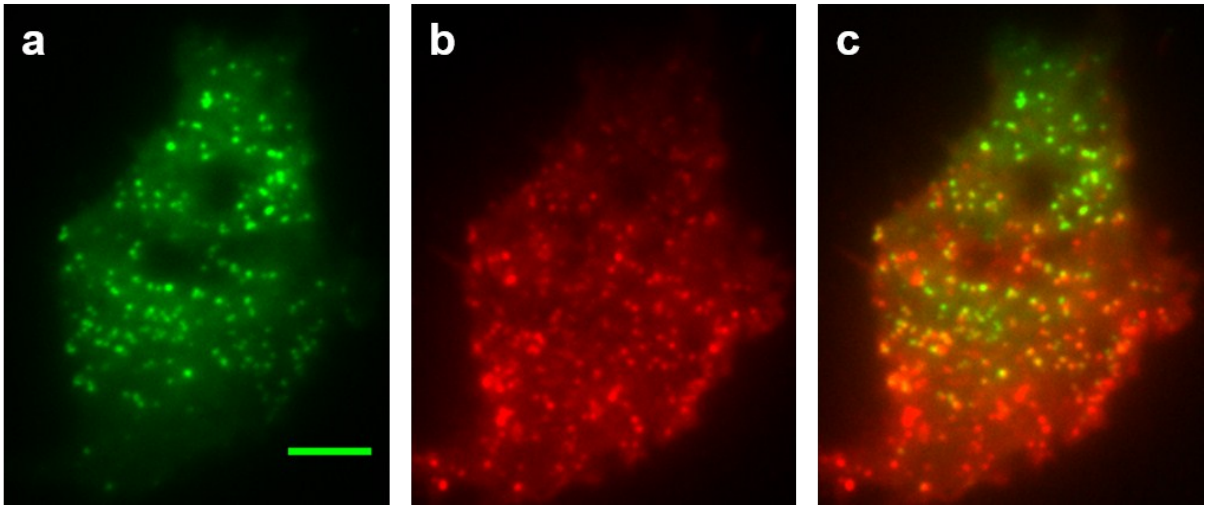

Fig. S14 Dual-color TIRF image of a COS-7 cell expressing CLC-mEos2, exposed to fluorescently labeled Tf. a, Image taken in the green channel, showing the punctate structure of CLC-mEos2 CCPs. b, Image taken in the red channel, depicting Tf labeled with Alexa 647. c, Overlay image; the analysis yields a colocalization degree of ~37%. Scale bar, 5 μm.

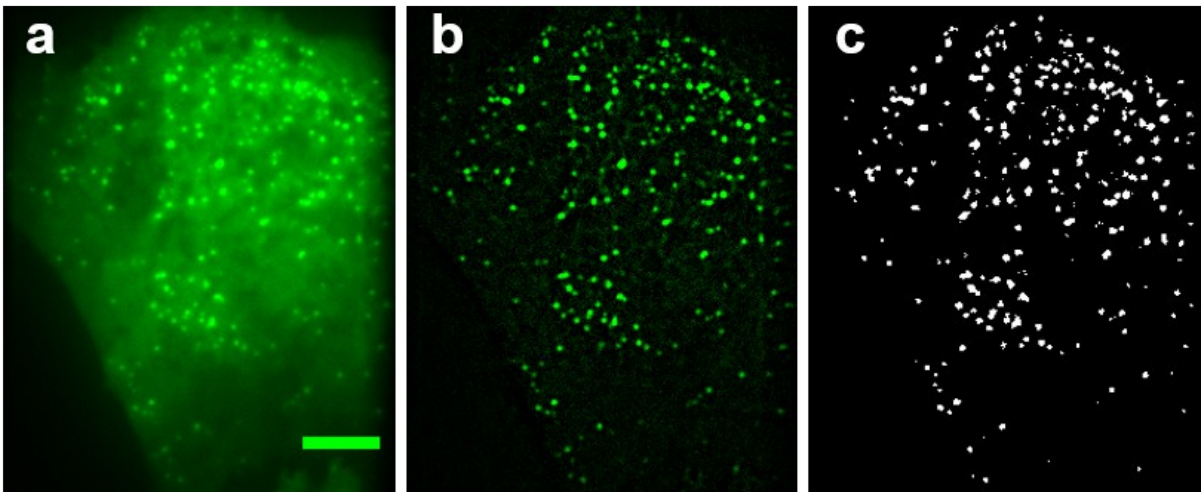

Fig. S15 Object extraction from TIRF images of COS-7 cells using ImageJ. a, TIRF microscopy image showing CCPs stained with CLC-mEos2. b, Image after background subtraction using a rolling ball algorithm with a ball size of 2 pixels. c, Objects (*i.e.*, clusters of 5 pixels or more) were extracted from the background-subtracted image by using the JACoP plugin. To calculate the fraction of CCPs colocalized with Tf clusters, this method was applied to both CLC-mEos2 and Tf-Alexa647 images. Scale bar, 5 μm.

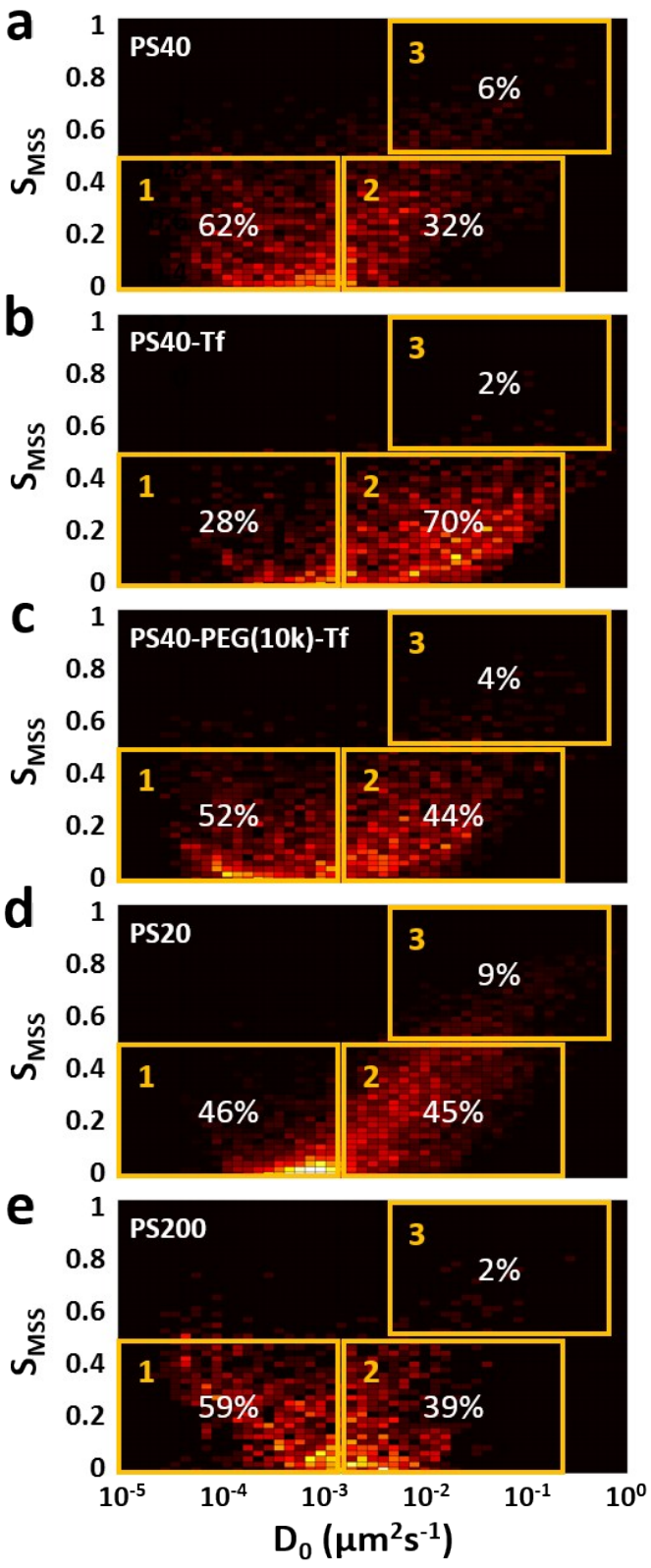

Fig. S16 Analysis of PS NP dynamics on COS-7 cell membranes using S_{MSS} versus D_0 plots. The diffusion coefficient D(t) at 1 s, D_0, was used to quantify the mobility from the trajectories, and the slope of the moment scaling spectrum (S_{MSS}) was used to characterize the

mode of movement. Three modes of motion could be distinguished: (i) confined diffusion (D_0 < 2 × 10^{-3} μm^2 s^{-1}, box 1); (ii) fast random diffusion with transient confinement (D_0 > 2 × 10^{-3} μm^2 s^{-1}, S_{MSS} < 0.5, box 2); (iii) directed movement (S_{MSS} > 0.5, box 3). The three boxes highlight regions in the graph in which NP motion is confined (box 1), rapid with transient confinement (box 2) or directed (box 3); the corresponding fractions are given in the boxes. a, PS40 NPs, b, PS40-Tf NPs, c, PS40-PEG(10k)-Tf NPs, d, PS20 NPs and e, PS200 NPs.

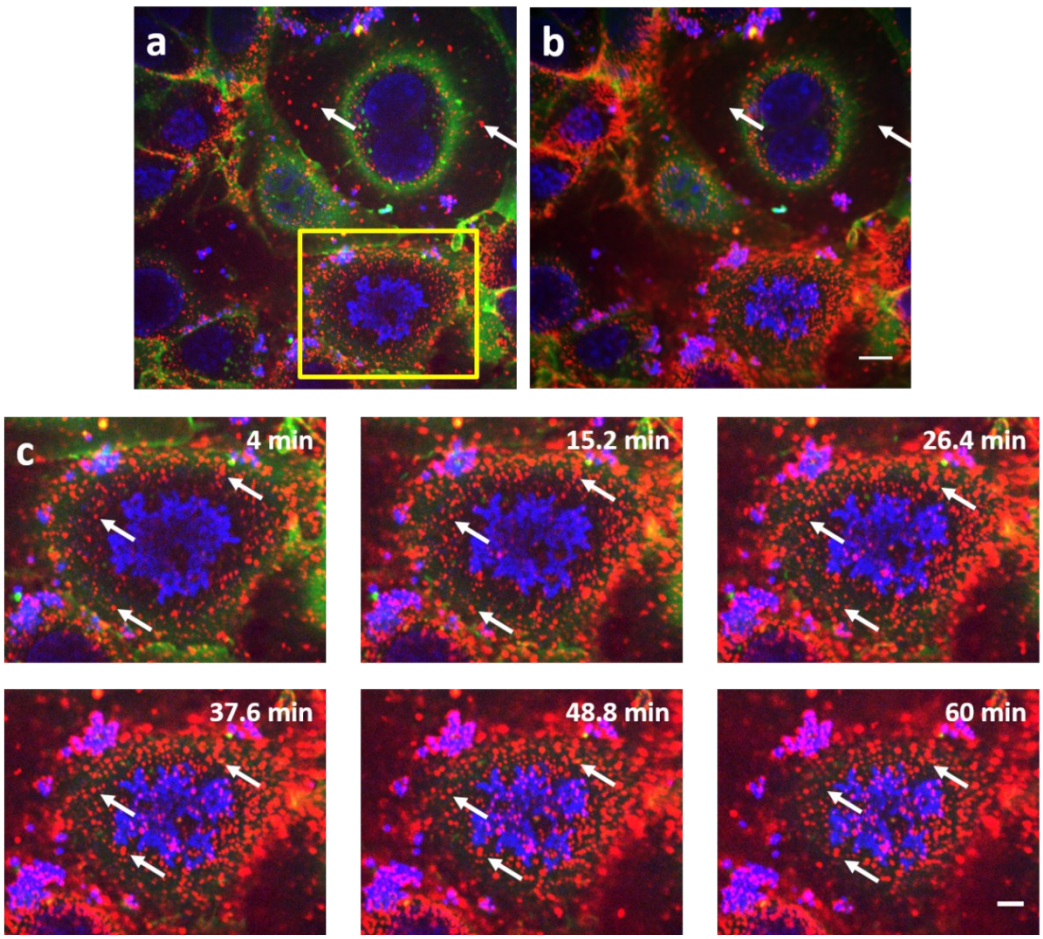

Fig. S17 Multi-color spinning disk confocal images of COS-7 cells exposed to PS40 NPs, taken in three color channels. Blue: nucleus (Hoechst 33342); green: plasma membrane (CellMask™ Orange); red: PS40 NPs. a, Single confocal image scanned at the height level of the top membrane of the cell marked by the yellow frame. b, Integrated image of all camera frames collected during 1 h in 2 s intervals (50 ms exposure time); scale bar, 10 µm. The white arrows mark locations where NPs identified in panel a are not visible in panel b, indicating that these are fast-moving NPs diffusing in the cell medium. By contrast, many spots on the plasma membrane of the marked cell in the first image (panel a) are still visible in the 1-h integrated image, indicating their low mobility. c, Temporal evolution of the marked region of panel a; scale bar, 5 µm. Evidently, many PS40 NPs at the top membrane can be tracked over long times, as was observed for the basal membrane. They are apparently bound to CCPs and confined to small membrane regions, likely due to a "fence" or ''corral" formed by cortical actin that restricts long-range diffusion.[10, 11]

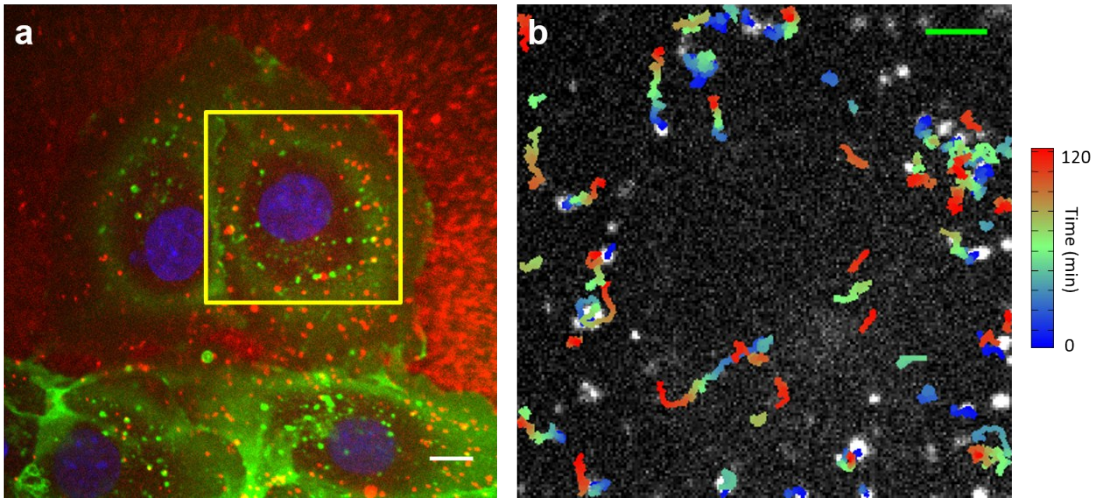

Fig. S18 Multi-color spinning disk confocal imaging of PS40-PEG(10k)-Tf NPs on COS-7 cells. Blue: nucleus (Hoechst 33342); green: membrane (CellMask™ Orange); red: PS40 NPs. a, Confocal image of PS40-PEG(10k)-Tf NPs across the top cell surface; scale bar 10 µm. b, NP trajectories longer than 5 min in the region marked by the yellow frame in panel a over 2 h; scale bar 5 µm.

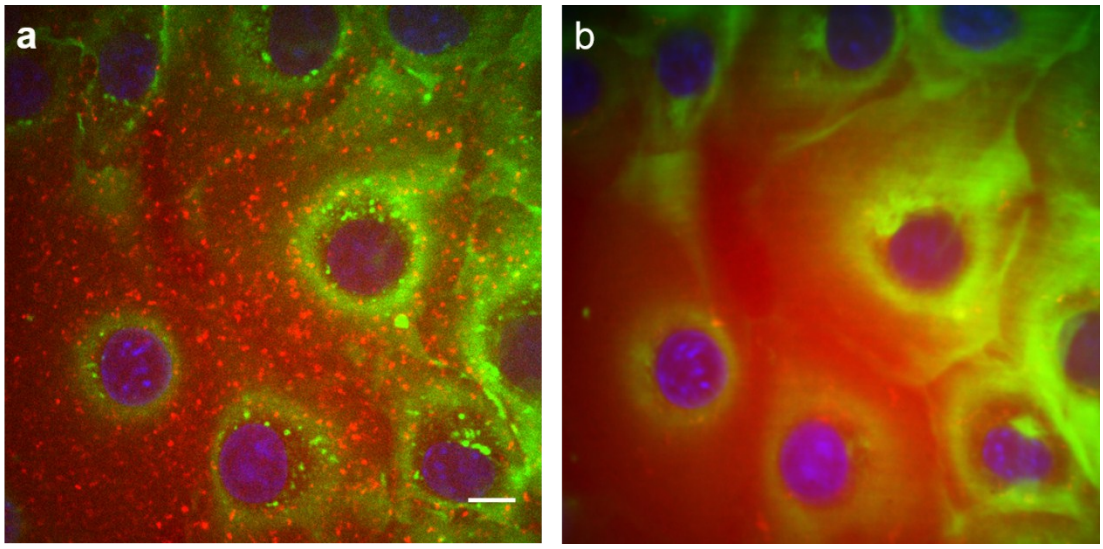

Fig. S19 Multi-color spinning disk confocal imaging of PS40-Tf NPs on COS-7 cells. Blue: nucleus (Hoechst 33342); green: membrane (CellMask™ Orange); red: PS40 NPs. a, Confocal image of PS40-Tf NPs scanned across the top cell surface, showing NPs as punctate structures; scale bar, 10 μm. b, Integrated image of all camera frames (50 ms exposure time) collected during 2 h in 30 s intervals; resident spots are essentially absent, indicating that these NPs are not immobilized by tightly adhering to the membrane, confirming the observations made by single particle tracking.

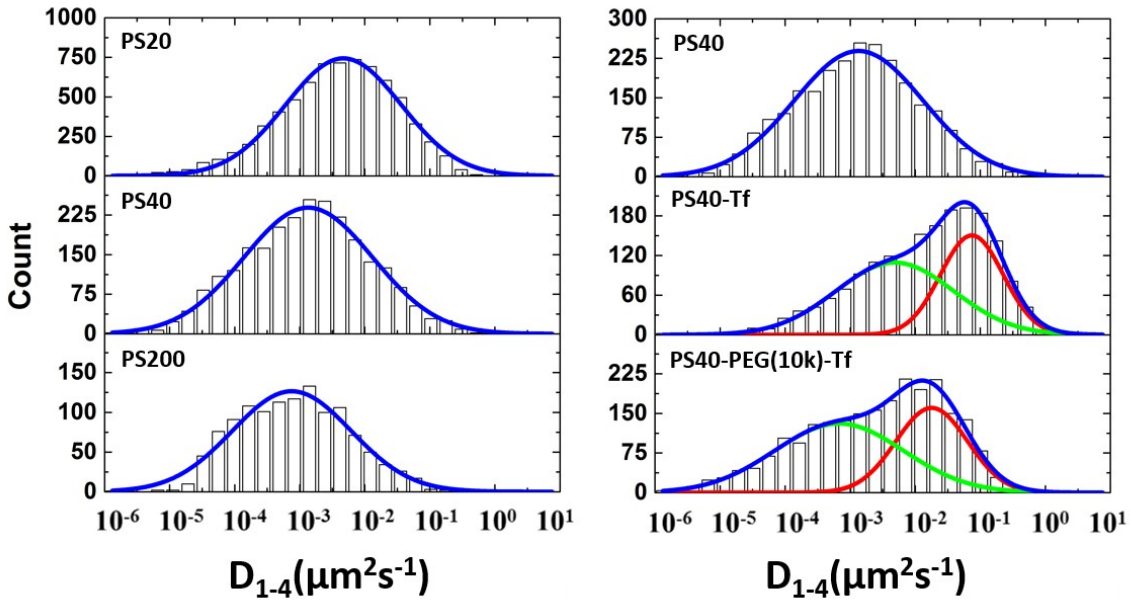

Fig. S20 Histograms of trajectory counts versus microscopic diffusion coefficient $D_{1\text{-}4}$ for different PS NPs. Left column: Histogram data and fits with log-normal functions, centered on 4.8×10^{-3} μm^2 s^{-1}, 1.3×10^{-3} μm^2 s^{-1} and 0.8×10^{-3} μm^2 s^{-1} for PS20, PS40 and PS200, respectively, indicating that the $D_{1\text{-}4}$ distributions shift to lower values with increasing size of the PS NPs. Right column: Histogram data and fits with one or a sum of two log-normal functions for PS40 NPs, PS40-Tf NPs and PS40-PEG(10k)-Tf NPs. For PS40-Tf NPs, two populations were identified from fitting with a sum of two log-normal functions centered on 0.5×10^{-2} μm^2 s^{-1} and 0.8×10^{-1} μm^2 s^{-1}. Likewise, for PS40-PEG(10k)-Tf NPs, there were also two distinct populations, centered on 0.7×10^{-3} μm^2 s^{-1} and 1.8×10^{-2} μm^2 s^{-1}.

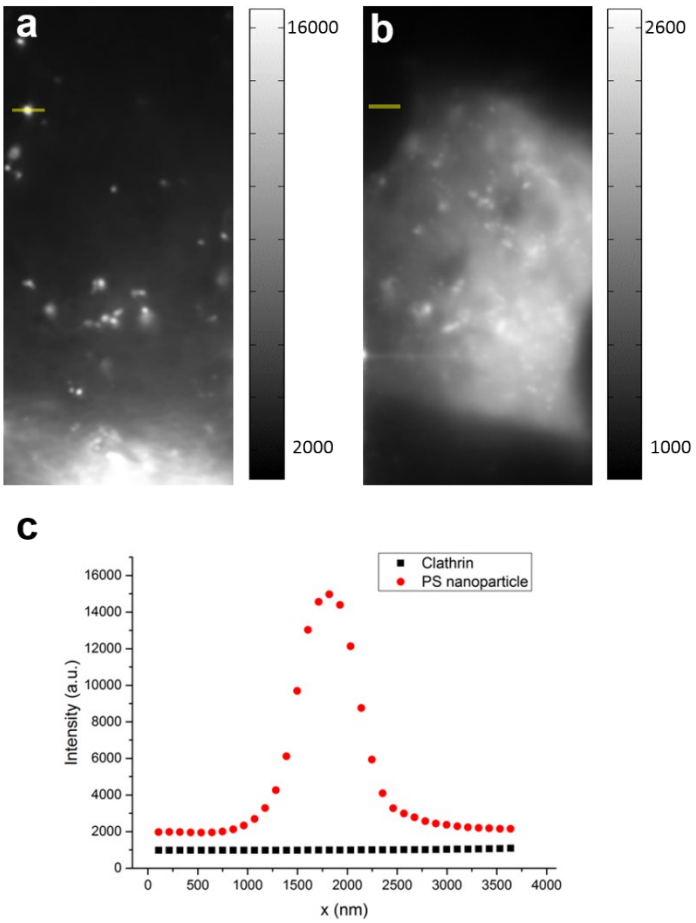

Fig. S21 Raw two-color TIRF image of a CLC-mEos2 expressing COS-7 cell exposed to PS40 NPs. PS40 NPs and CCPs were simultaneously imaged on the EMCCD camera in two color channels. Average of 4,086 images in, a, the PS40 NPs channel and, b, CLC-mEos2 channel. c, Fluorescence intensity plot of cross sections (500 nm wide) through the same position in the PS40 NPs channel (yellow line in a) and the CLC-mEos2 channel (yellow line in b), clearly showing that crosstalk between the two channels is negligible. The bars on the right sides of panels a and b show the mapping of the grey scales to intensity.

Description of Supporting Movies

Movie S1 Time-lapse PALM movie of CCPs shown in Fig 3a. 500 frames (15 s) were used to reconstruct one movie frame, and the time interval between successive images was 50 frames (1.5 s). The center of the CCP moved in the same direction as the PS40 NPs (Fig. 2b).

Movie S2 Spinning disk imaging of the interaction between a COS-7 cell and PS40 NPs. Red: PS40 NPs, green: cell membrane, blue: nucleus.

Movie S3 Spinning disk imaging of the interaction between a COS-7 cell and PS40-Tf NPs. Red: PS40-Tf NPs, green: cell membrane, blue: nucleus.

Movie S4 Spinning disk imaging of the interaction between a COS-7 cell and PS40-PEG(10k)-Tf NPs. Red: PS40-PEG(10k)-Tf NPs, green: cell membrane, blue: nucleus.

References:

1. X. Jiang, C. Röcker, M. Hafner, S. Brandholt, R. M. Dörlich and G. U. Nienhaus, *ACS Nano*, 2010, **4**, 6787-6797.
2. Y. Li, Y. Ishitsuka, P. N. Hedde and G. U. Nienhaus, *ACS Nano*, 2013, **7**, 5207-5214.
3. A. Goshtasby, *Image Vis. Comput.*, 1988, **6**, 255-261.
4. C. S. Smith, N. Joseph, B. Rieger and K. A. Lidke, *Nat. Methods*, 2010, **7**, 373-375.
5. R. Ferrari, A. J. Manfroi and W. R. Young, *Phys. D Nonlinear Phenom.*, 2001, **154**, 111-137.
6. H. Ewers, A. E. Smith, I. F. Sbalzarini, H. Lilie, P. Koumoutsakos and A. Helenius, *Proc. Natl. Acad. Sci. U.S.A.*, 2005, **102**, 15110-15115.
7. A. Kusumi, Y. Sako and M. Yamamoto, *Biophys. J.*, 1993, **65**, 2021-2040.
8. Z. Wang, C. Tiruppathi, R. D. Minshall and A. B. Malik, *ACS Nano*, 2009, **3**, 4110-4116.
9. A. Kusumi, C. Nakada, K. Ritchie, K. Murase, K. Suzuki, H. Murakoshi, R. S. Kasai, J. Kondo and T. Fujiwara, *Annu. Rev. Biophys. Biomol. Struct.*, 2005, **34**, 351-378.
10. Y. Sako and A. Kusumi, *J. Cell Biol.*, 1994, **125**, 1251-1264.
11. T. Kirchhausen, *Trends Cell Biol.*, 2009, **19**, 596-605.